The Effect of Water Solubles on the Hygroscopicity of Urban Aerosols

B. I. Tijjani
Department of Physics, Bayero University, Kano. NIGERIA.

ABSTRACT
In this paper, the author extracted some microphysical and optical properties of urban aerosols from OPAC by varying the concentrations of water soluble at the spectral range of 0.25µm to 2.5µm and eight relative humidities (RHs) (0, 50, 70, 80, 90, 95, 98, and 99%).The microphysical properties extracted were diameters, volume mix ratio, number mix ratio, mass mix ratio and refractive indices while the optical properties are optical depth and asymmetric parameters all as a function of RHs. Using the microphysical properties, hygroscopic growth factors of the mixtures and their effective refractive indices were determined while using optical depth we determined its relation with RHs, the enhancement parameters and Angstrom parameters. The hygroscopic growths and enhancement parameters were then parameterized using some models to determine their relationship with RHs. The data fitted the models very well. The angstrom coefficients show that the mixtures have bi-modal type of distribution with the dominance of fine mode particles and the mode sizes increase with the increase in water soluble concentrations and RH. The relation of optical depth with RH shows improvement with the increase in water soluble but decreases with the increase in wavelengths. The asymmetric parameters show that hygroscopic growth enhances forward scattering at smaller wavelengths.

KEYWORDS*: microphysical properties, optical properties, hygroscopic growth, enhancement parameters, Angstrom coefficients, spectral range, water soluble.*

I. INTRODUCTION

The ambient relative humidity changes the phase and microphysical and optical properties of hygroscopic atmospheric aerosols such as sulfates, nitrates and chlorides. These aerosols contribute the largest to the mass budget of fine atmospheric particles on a global basis [1-3]. These inorganic salt aerosols are hygroscopic by nature, thus their size, phase and subsequently the optical properties would be strongly influenced by their concentration and the ambient relative humidity (RH).As the ambient relative humidity (RH) changes, hygroscopic atmospheric aerosols undergo phase transformation, droplet growth, and evaporation. Phase transformation from a solid particle to a saline droplet usually occurs spontaneously when the RH reaches a level called the deliquescence humidity. Its value is specific to the chemical composition of the aerosol particle [4,5]. Since aerosols are far from being a single component, the question is how changes in relative humidity and changes in their concentrations influence the properties of natural aerosol mixtures, which can contain both soluble and insoluble components. Also most atmospheric aerosols are externally mixed with respect to hygroscopicity, and consist of more and less hygroscopic sub-fractions [6]. The ratio between these fractions as well as their content of soluble material determines the hygroscopic growth of the overall aerosol. In the natural environment the changes observed at a given wavelength are signs that measuring conditions have changed. These changes can be related either to an increase in RH or to a change in the aerosol concentration, though most often, both factors are present. Optical measurements at one single wavelength will not resolve the question whether the observed changes are caused only by the increased humidity or whether the additional aerosol particles have contributed to the changes. To be able to retrieve more accurate information about the aerosol mixtures, spectral measurements are needed.

The more spectral information available, the greater are the chances of getting a more realistic idea of the aerosol composition. To model droplet growth, information about water activity and density as a function of solute concentration is needed. The chemical and physical characteristics of aerosols are diverse and attempting to encompass such variability within a hygroscopic model is complex. By taking up water, particles grow in size

and experience modifications to their refractive indices, which change their ability to interact with solar radiation. An aerosol may exist in a solid or liquid state or a combination of the two over a wide range of ambient conditions both in the sub and super saturated humid environment [7-10]. Thus, where possible, the ability to couple the chemical and physical characteristics to the equilibrium phase of the aerosol is the ultimate aim of any hygroscopic modeling approach. The cloud droplets and water in deliquesced aerosol particles provide an aqueous medium for chemical reactions, which can lead to a change in the chemical composition of the particles [11-15]. Additionally, depending on the chemical and physical compositions, aerosol hygroscopic growth with increasing relative humidity (RH) may lead to dramatic changes in its mass concentration, size distribution and corresponding optical properties, which could enhance the cooling effect of aerosols in the atmosphere by directly scattering more light radiation [16-20], or change cloud microphysical properties [21] by serving as cloud condensation nuclei (CCN) [22]. Particle hygroscopicity may vary as a function of time, place, and particle size [6,23,24]. Previous studies reported that different types of aerosol particles usually have distinct hygroscopic growth properties [25-27].Hand and Malm [28] indicated that the scattering coefficients of $(NH_4)_2SO_4$ and $(NH_4)HSO_4$ aerosols could be enhanced by a factor of three when relative humidity is over 85%. Dust particles, dominant in coarse mode, are mostly insoluble [29], but they could also be hygroscopic when coated by sulfate or other soluble inorganic aerosols during transportation [30,31].

The hygroscopicity, are currently modeled in global climate models (GCMs), mostly to better predict the scattering properties and size distribution under varying humidity conditions [32]. Measured and modeled enhancement factors have been described in several previous studies, including studies on urban [33,34].
Jeong et al. [35] demonstrated an exponential dependence of the aerosol optical thickness on relative humidity. A strong correlation of spectral aerosol optical thickness with precipitable water, especially for continental air masses, was shown by Rapti [36]. A weaker dependence was observed for air masses of maritime origin.
In this paper some microphysical and optical properties of urban aerosols were extracted from OPAC at the spectral wavelength of 0.25 to 2.50μm, at relative humidities of 0, 50, 70, 80, 90, 95, 98 and 99% and varying the concentrations of water soluble. The microphysical properties extracted are diameters of the aerosols, number mix ratios, volume mix ratio, mass mix ratio and refractive indices. They were used to determine the hygroscopic and the effective refractive indices. The optical properties extracted are optical depth and asymmetric parameters. The optical depth was used to determine the angstrom parameters using power law and enhancement parameters. The angstrom coefficients are used determine the particles' type and the type mode size distributions. One and two parameter models were used to determine the relationship between the enhancement parameter and hygroscopic growth with RH. The asymmetric parameters are used to determine the effects of hygroscopic growth and concentration of water soluble on forward scattering. The relationship between optical depth and RH was also determined as done by Jeong et al. [35] and Rapti[36].

II. METHODOLOGY

The models extracted from OPAC are given in table 1.

Table 1 Compositions of aerosols types [37].

Components	**Model A (N_i,cm^{-3})**	**Model B (N_i,cm^{-3})**	**Model C (N_i,cm^{-3})**
Insoluble	1.50	1.50	1.50
water soluble	15,000.00	25,000.00	35,000.00
Soot	130,000.00	130,000.00	130,000.00
Total	**145,001.50**	**155,001.50**	**165,001.50**

Where (N_i,cm^{-3}) is the number of particles cm^{-3}, water soluble components, consist of scattering aerosols, that are hygroscopic in nature, such as sulfates and nitrates present in anthropogenic pollution, while water insoluble and soot are not soluble in water and therefore the particles are assumed not to grow with increasing relative humidity.
The aerosol's hygroscopic growth factor gf(RH), [6,20] is defined as:

$$gf(RH) = \frac{D(RH)}{D(RH=0)} \qquad (1)$$

where RH is taken for seven values 50%, 70%, 80%, 90%, 95%, 98% and 99%. But since natural aerosols consist of mixtures of both the soluble and insoluble components, and more and less hygroscopic sub fractions, so information on the hygroscopicity modes was merged into an "over-all" hygroscopic growth factor of the mixture, gf_{mix}(RH), representative for the entire particle population as:

$$gf_{mix}(RH) = (\sum_k x_k gf_k^3)^{1/3} \qquad (2)$$

where the summation is performed over all compounds present in the particles and x_k represent their respective volume fractions, using the Zdanovskii-Stokes-Robinson relation [38-41]. Solute-solute interactions are neglected in this model and volume additivity is also assumed. The model assumes spherical particles, ideal mixing (i.e. no volume change upon mixing) and independent water uptake of the organic and inorganic components.
Equation (2) was also computed using the x_k as the corresponding number fractions [42,43].
We finally proposed the x_k to represent the mass mix ratio of the individual particles though since mass and volume are proportional, but this will enable us to see the effect of hygroscopic growth on the density of the mixture.
The RH dependence of $gf_{mix}(RH)$ can be parameterized in a good approximation by a one-parameter equation[44] as:

$$gf_{mix}(a_w) = \left(1 + \kappa \frac{a_w}{1-a_w}\right)^{\frac{1}{3}} \quad (3)$$

Here, a_w is the water activity, which can be replaced by the relative humidity RH, if the Kelvin effect is negligible, as for particles with sizes more relevant for light scattering and absorption. Particle hygroscopicity is a measure that scales the volume of water associated with a unit volume of dry particle [44] and depends on the molar volume and the activity coefficients of the dissolved compounds [45]. The coefficient κ is a simple measure of the particle's hygroscopicity and captures all solute properties (Raoult effect), that is it is for the ensemble of the particle which can be defined in terms of the sum of its components. The κ values derived for particles of a given composition may vary, depending upon the size, the concentration and RH it is derived at. The following sub-divisions at 85% RH were made by Liu et al., [46]; as: nearly-hydrophobic particles (NH):κ<=0.10 (gf_{mix}<=1.21), less-hygroscopic particles (LH): κ=0.10–0.20 (gf_{mix}=1.21–1.37); more-hygroscopic particles (MH): κ>0.20 (gf_{mix}>1.37).
The humidograms of the ambient aerosols obtained in various atmospheric conditions showed that $gf_{mix}(RH)$ could as well be fitted well with a γ-law [47-51] as

$$gf_{mix}(RH) = \left(1 - \frac{RH}{100}\right)^{\gamma} \quad (4)$$

The bulk hygroscopicity factor B under sub saturation RH conditions was determined using the relation:

$$B = (1 - gf_{mix}^3) ln a_w \quad (5)$$

where a_w is the water activity, which can be replaced by the RH as explained before. The equation can be described as the rate of absorption of water of the bulk mixture as the RH increases.
The impact of hygroscopic growth on the aerosol optical depth is usually described by the enhancement factor $f_\tau(RH, \lambda)$:

$$f_\tau(RH, \lambda) = \frac{\tau(RH, \lambda)}{\tau(RH=0, \lambda)} \quad (6)$$

where RH is taken for seven values 50%, 70%, 80%, 90%, 95%, 98% and 99%.
In general the relationship between $f_\tau(RH, \lambda)$ and RH is nonlinear [35]. In this paper we determine the empirical relations between the enhancement parameter and RH [52] as:

$$f_\tau(RH, \lambda) = \frac{\tau(RH, \lambda)}{\tau(RH_{ref}, \lambda)} = \left(\frac{100 - RH_{ref}}{100 - RH_{high}}\right)^{\gamma} \quad (7)$$

where in our study RH_{ref} was 0%, and RH_{high} was taken for seven values 50%, 70%, 80%, 90%, 95%, 98% and 99%. The γ known as the humidification factor represents the dependence of aerosol optical properties on RH, which results from changes in the particle size and refractive index upon humidification. The use of γ has the advantage of describing the hygroscopic behavior of aerosols in a linear manner over a broad range of RH values; it also implies that particles are deliquesced [53], a reasonable assumption for this data set due to the high ambient relative humidity during the field studies. The γ parameter is dimensionless, and it increases with increasing particle water uptake. From previous studies, typical values of γ for ambient aerosol ranged between 0.1 and 1.5 [53-55] .
Two parameters empirical relation was also used [35,56] as;

$$f_\tau(RH, \lambda) = a\left(1 - \frac{RH(\%)}{100}\right)^{b} \quad (8)$$

Equations (7) and (8) were determined at wavelengths 0.25, 0.45, 0.55, 0.70, 1.25, and 2.50μm.
To determine the effect of particles mode distributions as a result of change in RH and water soluble, the Angstrom exponent was determined using the spectral behavior of the aerosol optical depth, with the wavelength of light (λ) was expressed as inverse power law [57]:

$$\tau(\lambda) = \beta\lambda^{-\alpha} \quad (9)$$

The Angstron exponent was obtained as a coefficient of the following regression,

$$ln\tau(\lambda) = -\alpha ln(\lambda) + ln\beta \quad (10)$$

However equation (10) was determined as non-linear (that is the Angstrom exponent itself varies with wavelength), and a more precise empirical relationship between the optical depth and wavelength was obtained with a 2nd-order polynomial [58-68] as:

$$\ln\tau(\lambda)=\alpha_2(\ln\lambda)^2 + \alpha_1\ln\lambda + \ln\beta \quad (11)$$

We then proposed the cubic relation to determine the type of mode distribution as:

$$\ln\tau(\lambda)= \ln\beta + \alpha_1\ln\lambda + \alpha_2(\ln\lambda)^2+ \alpha_3(\ln\lambda)^3 \quad (12)$$

where β, α, α_1, α_2, α_3 are constants that were determined using regression analysis with SPSS16.0 for windows. Equations (10), (11) and (12) were evaluated at eight RHs for the corresponding change in water soluble concentrations.

We also determined an exponential dependence of the aerosol optical thickness on relative humidity as done by Jeong et al. [35] as;

$$\tau(RH) = Ae^{B(RH/100)} \quad (13)$$

where A and B are constants determined using regression analysis with SPSS 16.0 for windows. The relationship was determined at 0.25μm, 1.25μm and 2.50μm.

We finally determined the effect of hygroscopic growth and the change in the concentration of water soluble on the effective refractive indices of the mixed aerosols using the formula [69]:

$$\frac{\varepsilon_{eff}-\varepsilon_0}{\varepsilon_{eff}+2\varepsilon_0} = \sum_{i=1}^{3} f_i \frac{\varepsilon_i-\varepsilon_0}{\varepsilon_i+2\varepsilon_0} \quad (14)$$

where f_i and ε_i are the volume fraction and dielectric constant of the i^{th} component and ε_0 is the dielectric constant of the host material.

The relation between dielectrics and refractive indices is

$$m_i = \sqrt{\varepsilon_i} \quad (15)$$

For the case of Lorentz-Lorentz [70,71], the host material is taken to be vacuum, ε_0 =1.

The computation of equations (14) and (15) was done using the complex functions of Microsoft Excel 2010.

III. RESULTS AND DISCUSSIONS

Table 2a: the growth factors of the aerosols using number mix ratio (equation 2) and Bulk hygroscopicity factor (equation 5) for Model A.

RH(%)	50	70	80	90	95	98	99
$gf_{mix}(RH)$	1.0297	1.0470	1.0649	1.1063	1.1661	1.0538	1.3660
B	0.0635	0.0527	0.0463	0.0373	0.0301	0.0034	0.0156

Table 2b: the growth factors of the aerosols using number mix ratio (equation 2) *and Bulk hygroscopicity factor (equation 5) for Model B.*

RH(%)	50	70	80	90	95	98	99
$gf_{mix}(RH)$	1.0456	1.0716	1.0980	1.1578	1.2416	1.3863	1.5061
B	0.0992	0.0822	0.0722	0.0582	0.0469	0.0336	0.0243

Table 2c: the growth factors of the aerosols using number mix ratio (equation 2) *and Bulk hygroscopicity factor (equation 5) for Model C.*

RH(%)	50	70	80	90	95	98	99
$gf_{mix}(RH)$	1.0592	1.0923	1.1255	1.1995	1.3010	1.4719	1.6106
B	0.1305	0.1082	0.0950	0.0765	0.0617	0.0442	0.0319

Tables 2a, 2b and 2c show that there is an increase in both $gf_{mix}(RH)$ and B with the increase in the concentrations of water soluble. It can also be observed the hygroscopic growth has caused increased in $gf_{mix}(RH)$ but decrease in B.

The data from tables 2a, 2b and 2c were applied for the parametrisations of equations (3) and (4). The results obtained are as follows:

The results of the parameterizations by one parameter of equations (3) and (4) for Model A are:

k=0.0175, $R2$=0.9470 using equation (3)

γ=-0.0588, $R2$=0.9731 using equation (4)

The results of the parameterizations by one parameter of equations (3) and (4) for Model B are:

k=0.0272, $R2$=0.9470 using equation (3)

γ=-0.0798, $R2$=0.9834 using equation (4)

The results of the parameterizations by one parameter of equations (3) and (4) for Model C are:
k=0.0358, $R2$=0.9470 using equation (3)
γ=-0.0949, $R2$=0.9891 *using* equation (4)
From the observations of R^2 it can be seen that the data fitted the equations very well (equations 3 and 4). It can also be observed that hygroscopicity of the mixtures (k) and γ using γ-law, all increase with the increase in the concentrations of water solubles.

Table 3a: the growth factors of the aerosols using volume mix ratio (equation 2) *and Bulk hygroscopicity factor (equation 5) for Model A.*

RH(%)	50	70	80	90	95	98	99
gf_{mix}(RH)	1.1190	1.2019	1.2886	1.4822	1.7346	2.1242	2.4162
B	0.2781	0.2626	0.2544	0.2377	0.2164	0.1734	0.1317

Table 3b: the growth factors of the aerosols using volume mix ratio (equation 2) *and Bulk hygroscopicity factor (equation 5) for Model B.*

RH(%)	50	70	80	90	95	98	99
gf_{mix}(RH)	1.1482	1.2415	1.3348	1.5344	1.7862	2.1689	2.4550
B	0.3561	0.3259	0.3075	0.2753	0.2410	0.1859	0.1387

Table 3c: the growth factors of the aerosols using volume mix ratio (equation 2) *and Bulk hygroscopicity factor (equation 5) for Model C.*

RH(%)	50	70	80	90	95	98	99
gf_{mix}(RH)	1.1657	1.2638	1.3597	1.5607	1.8111	2.1895	2.4725
B	0.4048	0.3633	0.3377	0.2952	0.2534	0.1919	0.1419

Tables 3a, 3b and 3c show that there is an increase in both gf_{mix}(RH) and B with the increase in the concentrations of water soluble. It can also be observed the hygroscopic growth has caused increased in gf_{mix}(RH) but decrease in B.

The data from tables 3a, 3b and 3c were applied for the parametrisations of equations (3) and (4). The results obtained are as follows:
The results of the parameterizations by one parameter of equations (3) and (4) for Model A are:
k=0.1441, $R2$=0.9729 using equation (3)
γ=-0.1857, $R2$=0.9966 using equation (4)
The results of the parameterizations by one parameter of equations (3) and (4) for Model B are:
k=0.1530, $R2$=0.9658 using equation (3)
γ=-0.1936, $R2$=0.9993 using equation (4)
The results of the parameterizations by one parameter of equations (3) and (4) for Model C are:
k=0.1572, $R2$=0.9618 using equation (3)
γ=-0.1975, $R2$=0.9997 using equation (4)
From the observations of R^2 it can be seen that the data fitted the equations very well (equations 3 and 4). It can also be observed that hygroscopicity of the mixtures (k) and γ using γ-law, all increase with the increase in the concentrations of water solubles.

Table 4a: the growth factors of the aerosols using mass mix ratio (equation 2) *and Bulk hygroscopicity factor (equation 5) for Model A.*

RH(%)	50	70	80	90	95	98	99
gf_{mix}(RH)	1.1086	1.1816	1.2590	1.4364	1.6785	2.0657	2.3614
B	0.2512	0.2317	0.2221	0.2069	0.1913	0.1579	0.1223

Table 4b: the growth factors of the aerosols using mass mix ratio (equation 2) *and Bulk hygroscopicity factor (equation 5) for Model B.*

RH(%)	50	70	80	90	95	98	99
gf_{mix}(RH)	1.1383	1.2233	1.3098	1.4988	1.7457	2.1294	2.4191
B	0.3291	0.2963	0.2783	0.2494	0.2216	0.1749	0.1322

Table 4c: the growth factors of the aerosols using mass mix ratio (equation 2) *and Bulk hygroscopicity factor (equation 5)* for *Model C.*

RH(%)	50	70	80	90	95	98	99
$gf_{mix}(RH)$	1.1567	1.2480	1.3386	1.5321	1.7794	2.1597	2.4458
B	0.3796	0.3366	0.3121	0.2735	0.2377	0.1833	0.1370

Tables 4a, 4b and 4c show that there is an increase in both $gf_{mix}(RH)$ and B with the increase in the concentrations of water soluble. It can also be observed the hygroscopic growth has caused increased in $gf_{mix}(RH)$ but decrease in B.

The data from tables 4a, 4b and 4c were applied for the parametrisations of equations (3) and (4). The results obtained are as follows:

The results of the parameterizations by one parameter of equations (3) and (4) for Model A are:

k=0.1328, $R2$=0.9777 using equation (3)

γ=-0.1776, $R2$=0.9939 using equation (4)

The results of the parameterizations by one parameter of equations (3) and (4) for Model B are:

k=0.1451, $R2$=0.9701 using equation (3)

γ=-0.1879, $R2$=0.9983 using equation (4)

The results of the parameterizations by one parameter of equations (3) and (4) for Model C are:

k=0.1511, $R2$=0.9655 using equation (3)

γ=-0.1930, $R2$=0.9994 using equation (4)

From the observations of R^2 it can be seen that the data fitted the equations very well (equations 3 and 4). It can also be observed that hygroscopicity of the mixtures (k) and γ using γ-law, all increase with the increase in the concentrations of water solubles, though the γ-law shows inverse power laws.

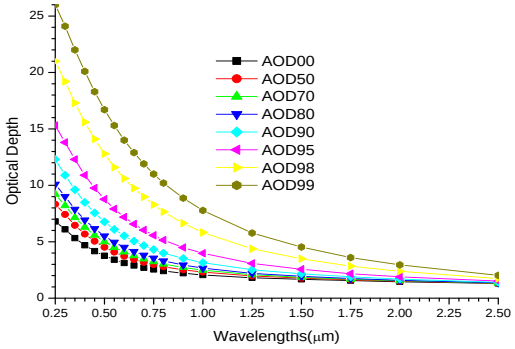

Figure 1a: A graph of optical depth against wavelengths for Model A.

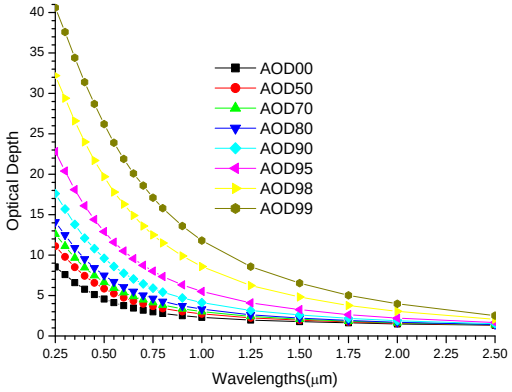

Figure 1b: A graph of optical depth against wavelengths for Model B.

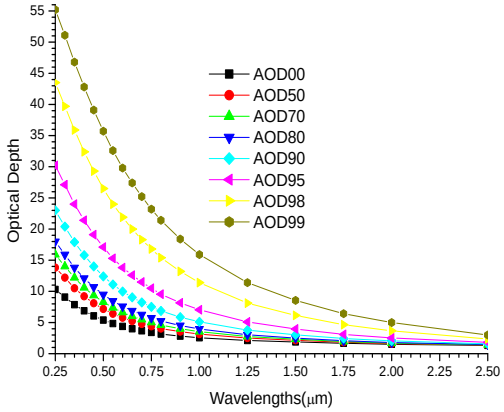

Figure 1c: A graph of optical depth against wavelengths for Model C.

From figures 1a, 1b and 1c, it can be observe that the optical depth follows a relatively smooth decrease with wavelength for all RHs and can be approximated with power law wavelength dependence. It is evident from the figures that there is relatively strong wavelength dependence of optical depth at shorter wavelengths that gradually decreases towards longer wavelengths irrespective of the RH and concentrations, attributing to the dominance of fine over coarse particles. The presence of a higher concentration of the fine-mode particles which are selective scatters enhance the irradiance scattering in shorter wavelength only while the coarse-mode particles provide similar contributions to the AOD at both wavelengths [72]. This also shows that hygroscopic growth has more effect on fine particles than coarse particles. The relation of optical depth with RH and water soluble concentrations are such that at the deliquescence point (90 to 99%) this growth with higher humidities increases substantially, making this process strongly nonlinear with relative humidity and the increase in the concentrations of water soluble [25,73].

The data that were used in plotting figures 1a, 1b and 1c were applied to equation (13), at the wavelengths of 0.25, 1.25 and 2.50μm. The results obtained are as follows:
The exponential relations (13) between optical depth and RHs for *Model A* are:
At λ=0.25μm, A=5.4740, B=1.1185, R^2= 0.6577
At λ=1.25 μ, A=1.4583, B=0.8678, R^2= 0.5022
At λ=2.50 μ, A=1.2070, B=0.2858, R^2= 0.3862
The relation between optical depth and RHs using equation (13) for *Model B* are:
At λ=0.25μ, A=6.7084, B=1.3187, R^2= 0.6856
At λ=1.25 μ, A=1.5039, B=1.1344, R^2= 0.5360
At λ=2.50 μ, A=1.1794, B=0.4350, R^2= 0.4124
The relation between optical depth and RHs for *Model C* using equation (13) are:
At λ=0.25μ, A=7.9690, B=1.4323, R^2= 0.6984
At λ=1.25 μ, A=1.5640, B=1.3222, R^2= 0.5602
At λ=2.50 μ, A=1.1593, B=0.5580, R^2=0.4273
The relation between optical depth and RH shows decrease in R^2 and the exponent B with the increase in wavelength but both increase with the increase in the concentrations of water solubles. This shows that the relation is better for fine particles.

Table 5a the results of the Angstrom coefficients for Model A using equations (10), (11) and (12) at the respective relative humidities using regression analysis with SPSS16 for windows.

RH	Linear equ(10)		Quadratic equ(11)			Cubic equ(12)			
(%)	R2	α	R2	α1	α2	R2	α1	α2	α3
0	0.9757	0.7485	0.9963	-0.6745	0.1610	0.9976	-0.7206	0.2136	0.0689
50	0.9861	0.8388	0.9967	-0.7796	0.1289	0.9986	-0.8417	0.1997	0.0929
70	0.9904	0.8819	0.9968	-0.8335	0.1054	0.9990	-0.9024	0.1840	0.1031
80	0.9936	0.9205	0.9970	-0.8839	0.0796	0.9993	-0.9576	0.1637	0.1102
90	0.9972	0.9909	0.9974	-0.9826	0.0182	0.9997	-1.0615	0.1082	0.1180
95	0.9963	1.0584	0.9981	-1.0887	-0.0661	0.9999	-1.1637	0.0194	0.1120
98	0.9862	1.1164	0.9992	-1.2035	-0.1897	1.0000	-1.2544	-0.1317	0.0760
99	0.9747	1.1283	0.9998	-1.2515	-0.2682	0.9999	-1.2773	-0.2387	0.0386

Table 5b *the results of the Angstrom coefficients for Model B using equations (10), (11) and (12) at the respective relative humidities using regression analysis with SPSS16 for windows.*

RH	Linear equ(10)		Quadratic equ(11)			Cubic equ(12)			
(%)	R2	α	R2	α1	α2	R2	α1	α2	α3
0	0.9849	0.8527	0.9965	-0.7899	0.1367	0.9985	-0.8549	0.2109	0.0973
50	0.9932	0.9635	0.9968	-0.9239	0.0863	0.9993	-1.0042	0.1779	0.1201
70	0.9958	1.0128	0.9971	-0.9885	0.0530	0.9996	-1.0732	0.1497	0.1267
80	0.9972	1.0545	0.9973	-1.0460	0.0186	0.9997	-1.1327	0.1176	0.1297
90	0.9967	1.1249	0.9979	-1.1514	-0.0577	0.9999	-1.2346	0.0372	0.1244
95	0.9914	1.1831	0.9988	-1.2528	-0.1518	1.0000	-1.3204	-0.0747	0.1011
98	0.9771	1.2168	0.9997	-1.3428	-0.2743	1.0000	-1.3733	-0.2395	0.0456
99	0.9644	1.2088	0.9999	-1.3666	-0.3436	0.9999	-1.3688	-0.3411	0.0033

Table 5c *the results of the Angstrom coefficients for Model C using equations (10), (11) and (12) at the respective relative humidities using regression analysis with SPSS16 for windows.*

RH	Linear equ(10		Quadratic equ(11			Cubic equ(12)			
(%)	R2	α	R2	α1	α2	R2	α1	α2	α3
0	0.9901	0.9353	0.9965	-0.8840	0.1117	0.9990	-0.9621	0.2009	0.1168
50	0.9961	1.0558	0.9970	-1.0340	0.0474	0.9996	-1.1240	0.1501	0.1346
70	0.9973	1.1064	0.9973	-1.1026	0.0081	0.9998	-1.1944	0.1128	0.1372
80	0.9973	1.1477	0.9976	-1.1621	-0.0314	0.9999	-1.2524	0.0717	0.1351
90	0.9944	1.2130	0.9984	-1.2654	-0.1141	1.0000	-1.3451	-0.0231	0.1193
95	0.9868	1.2599	0.9993	-1.3563	-0.2098	1.0000	-1.4127	-0.1454	0.0844
98	0.9711	1.2735	0.9999	-1.4229	-0.3252	1.0000	-1.4371	-0.3090	0.0212
99	0.9584	1.2519	0.9998	-1.4293	-0.3860	0.9999	-1.4153	-0.4020	-0.0209

First, from tables 5a, 5b and 5c, it can be observed that at each table there is an increase in α with the increase in RH and water solubles, except tables 5b and 5c where α decreased at 99% RH, and this shows that increase in the concentration of water soluble has lowered the delinquent point of the mixtures. This increase in α signifies the increase in mode size distribution of the particles. The decrease in α2 at the positive part (the decrease in the curvature) and becoming more negative in the negative part (the increase in the curvature) with the increase in RH and water solubles, reflects the increase in the concentrations of small particles as a result of nucleation, accumulation and sedimentation. The cubic part signifies the type of mode distributions as bi-modal with the dominance of fine mode particles.

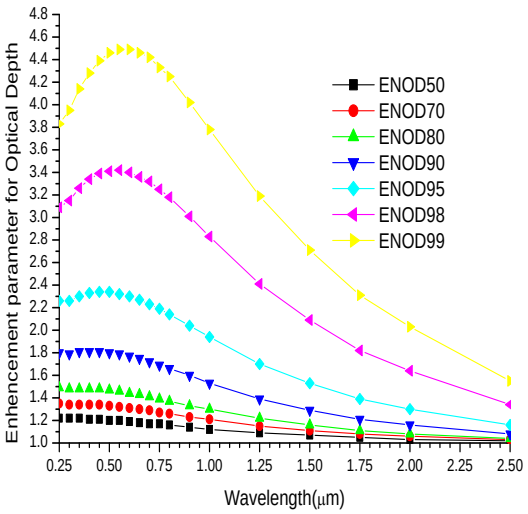

Figure 2a: A graph of enhancement parameter for optical depth against wavelengths for Model A

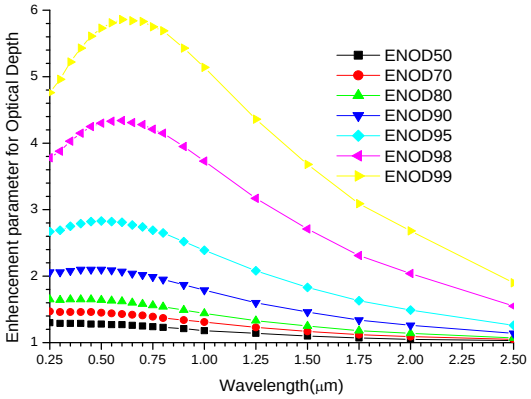

Figure 2b: A graph of enhancement parameter for optical depth against wavelengths for Model B.

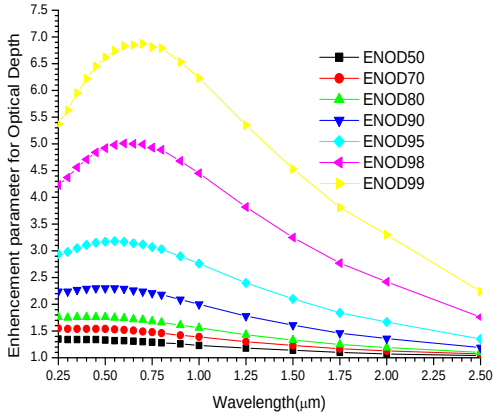

Figure 2c: A graph of enhancement parameter for optical depth against wavelengths for Model C

Figures 2a, 2b and 2c show that the enhancement factors increase both with the increase in RH and concentrations of water soluble in almost non-linear form. The most interesting phenomena is the visible range window (0.4 - 0.7 μm) and the near-infrared (0.7-1.0) where the enhancement is higher with both the increase in RH and the concentrations of water soluble. This shows that at this window the increase in the concentrations of water soluble can cause decrease in cloud cover, and/or reflective aerosol, this can cause decrease in global albedo, can result in the increase in energy input into Earth/Atmosphere system and finally can cause warming effect. That is it allows most solar radiation through to the surface and enables solar radiation to "deliver" the bulk of its energy to the surface (for use in climate processes)

The data that were used in plotting figures 2a, 2b and 2c were applied for the parametrisations of equations (7) and (8), at the wavelengths of 0.25, 0.45, 0.55, 0.70, 1.25 and 2.50μm. The results obtained are as follows:
The results of the fitted curves of equations (7) and (8) for *Model A* are presented as follows;

For a single parameter using equation (7).
At λ=0.25μ, γ=0.2809, R^2=0.9974
At λ=0.45μ, γ=0.3002, R^2= 0.9925
At λ=0.55 μ, γ=0.9925, R^2=0.9898
At λ=0.70 μ, γ=0.2922, R^2=0.9849
At λ=1.25 μ, γ=0.2113, R^2=0.9575
At λ=2.50 μ, γ=0.0701, R^2=0.8914

For two parameters using equation (8).
At λ=0.25μ, a=1.2062, b=-0.2985, R^2= 0.9940
At λ=0.45μ, a=1.4255, b=-0.3377, R^2=0.9895
At λ=0.55 μ, a=1.5132, b=-0.3460 , R^2=0.9873
At λ=0.70 μ, a=1.6466, b=-0.3462, R^2= 0.9834
At λ=1.25 μ, a=2.1526, b=-0.2781, R^2= 0.9619
At λ=2.50 μ, a=2.8743, b=-0.1048, R^2= 0.9078
The results of the fitted curves of equations (7) and (8) for *Model B* are presented as follows;

For a single parameter using equation (7).
At λ=0.25μ, γ=0.9899, R^2=0.9883
At λ=0.45μ, γ=1.1033, R^2=0.9851
At λ=0.55 μ, γ=1.1248, R^2=0.9826
At λ=0.70 μ, γ=1.1132, R^2=0.9797
At λ=1.25 μ, γ=0.8462, R^2= 0.9777
At λ=2.50 μ, γ=0.4501, R^2=0.9192

For two parameters using equation (8).
At λ=0.25μ, a=0.6800, b=-0.8832, R^2= 0.9550
At λ=0.45μ, a=0.9693, b=-1.0926, R^2=0.9361
At λ=0.55 μ, a=1.0495, b=-1.1421, R^2=0.9294
At λ=0.70 μ, a=1.1000, b=-1.1474, R^2= 0.9214
At λ=1.25 μ, a=0.8195, b=-0.7966, R^2= 0.9012
At λ=2.50 μ, a=0.0279, b=-0.2122, R^2= 0.8794

The results of the fitted curves of equations (7) and (8) for *Model C*are presented as follows;
For a single parameter using equation (7).
At λ=0.25μ, γ=1.1004, R^2= 0.9896
At λ=0.45μ, γ=1.2472, R^2=0.9835
At λ=0.55 μ, γ=1.2822, R^2=0.9799
At λ=0.70 μ, γ=1.2857, R^2=0.9759
At λ=1.25 μ, γ=1.0045, R^2= 0.9744
At λ=2.50 μ, γ=0.5018, R^2= 0.9424

For two parameters using equation (8);
At λ=0.25μ, a=0.7975, b=-1.0276, R^2= 0.9549
At λ=0.45μ, a=1.1158, b=-1.2916, R^2=0.9362
At λ=0.55 μ, a=1.2100, b=-1.3637, R^2=0.9294
At λ=0.70 μ, a=1.2842, b=-1.3950, R^2=0.9214
At λ=1.25 μ, a=1.0923, b=-1.0331, R^2= 0.9013
At λ=2.50 μ, a=0.1013, b=-0.2922, R^2= 0.8797

For both the one and two parameters models, the values of the exponents increase with the increase in the construction of water soluble, andthey increased most at the solar spectral window (0.40 to 0.70μm). These signified increase in water uptake with the increase in the concentrations of water soluble.

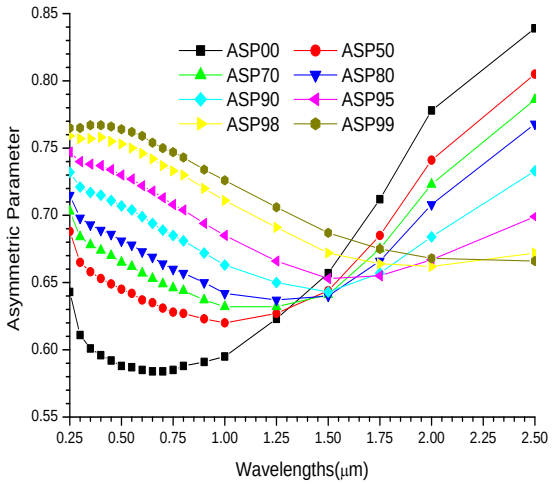

Figure 3a: A graph of Asymmetric parameter against wavelengths for *Model A*

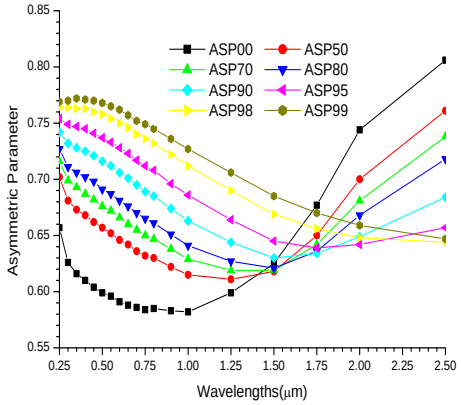

Figure 3b: A graph of Asymmetric parameter against wavelengths for Model B.

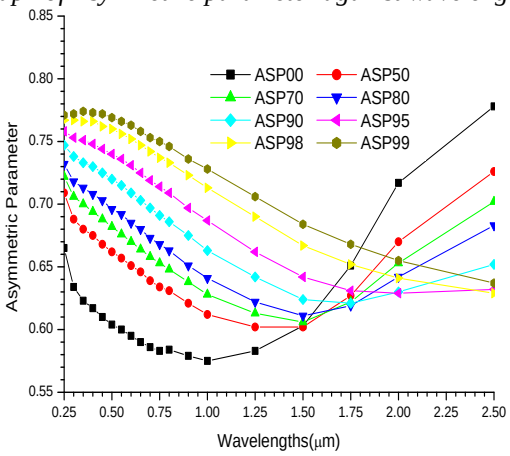

Figure 3c: A graph of Asymmetric parameter against wavelengths for Model C

Figures 3a, 3b and 3c show a slight increase in the asymmetric parameters with the increase in the concentration of water soluble. The increase with the increase in RH is faster at the solar spectral window. This shows that smaller particles enhance forward scattering with the increase in RH and water solubles.

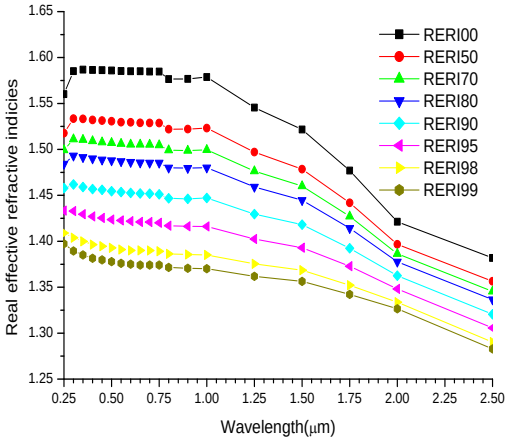

*Figure 4a: A plot of real effective refractive indices against wavelength using volume mix ratio*for *Model A.*

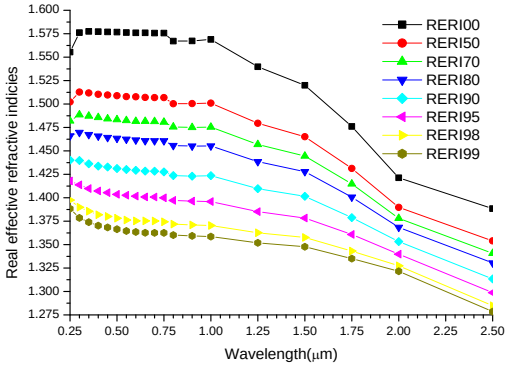

Figure 4b: A plot of real effective refractive indices against wavelength using volume mix ratio for *Model B.*

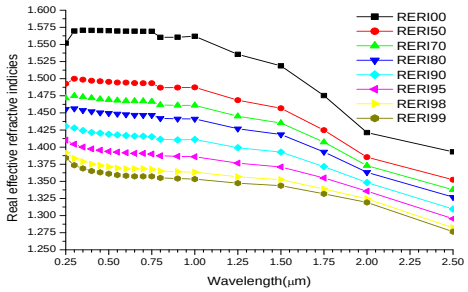

Figure 4c: A plot of real effective refractive indices against wavelength using volume mix ratio for *Model C.*

Figures 4a, 4b and 4c show decrease in the real effective refractive indices with increase in RH and water soluble. This signifies the reason why scattering increases with the increase in RH and water soluble. The linear relation decreases with the increase in wavelength.

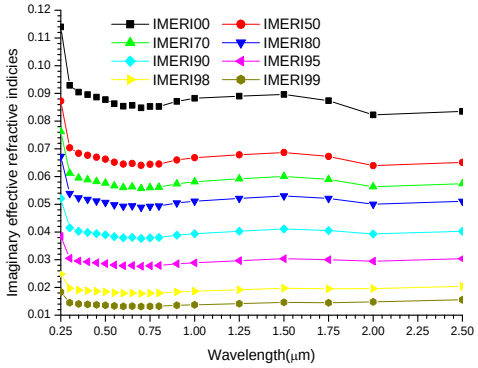

Figure 5a: A plot of imaginary effective refractive indices against wavelength using volume mix ratio for *Model A.*

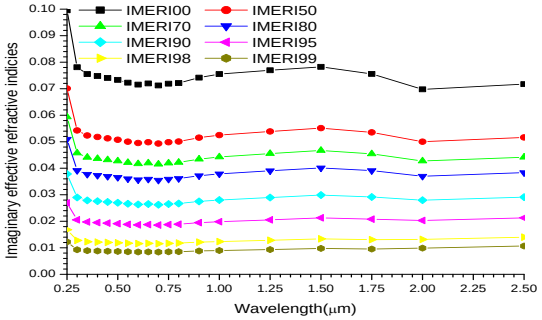

Figure 5b: A plot of imaginary effective refractive indices against wavelength using volume mix ratio for *Model B.*

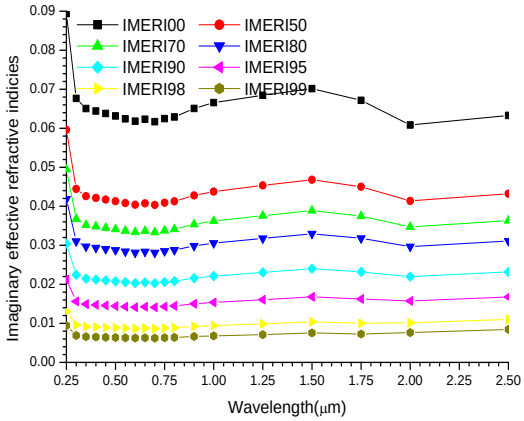

Figure 5c: A plot of imaginary effective refractive indices against wavelength using volume mix ratio for *Model C.*

Figures 5a, 5b and 5c show a slight decrease with the increase in RH and water soluble. This signifies decrease in absorption. It becomes more linear and constant with the increase in RH.

IV. CONCLUSIONS

In this paper we investigated the influence of relative humidity and soot on the microphysical and optical properties of atmospheric aerosol mixtures. The principal conclusions are:

[1] From the three $gf_{mix}(RH)$ it can be concluded that the higher values are observed using volume and mass mix ratios because of the high density of water soluble. This is in line with what Sheridan et al. [74] found, on the basis of analysis of in situ data collected at SGP in 1999, that aerosols containing higher fractions of smaller particles show larger hygroscopic growth factors. From our results despite soot being having the least size and higher in fractions, it shows that using volume mix and mass mix ratios, shows that the mixture is more hygroscopic. However, still in their studies, they also showed that aerosols containing higher fractions of more strongly absorbing particles exhibit lower hygroscopic growth factors, in our own case it shows that using number mix ratio. The importance of determining $gf_{mix}(RH)$ as a function of RH and volume fractions, mass fractions and number fractions, and enhancement parameters as a function of RH and wavelengths can be potentially important because it can be used for efficiently representing aerosols-water interactions in global models.

[2] Equation (3) with mass mix ratios has higher R^2 while equation (4) has higher values of R^2 using volume mix ratio. But since volume mix ratios gave higher values of $gf_{mix}(RH)$, k and γ, and the values of R2 are greater than 95%, it can be concluded that just as the optical effects of atmospheric aerosols are more closely related to their volume than their number [75,76], we discovered that the microphysical properties are also more closely related to their volume followed by mass. The increase in the values of $gf_{mix}(RH)$, k and γ with the increase in soot and water soluble concentration show that they increase hygroscopicity of aerosols.

[3] Changes in RH and soot and water soluble concentrations modified the optical properties not only of hygroscopic aerosol mixtures but also of mixtures containing non-hygroscopic aerosols like black carbon. As a result of wetting the hydroscopic particles grow, thereby changing the effective radius of the aerosol mixture and subsequently the aerosol extinction or aerosol optical thickness[77]. The changes are more substantial especially at the delinquent points where the hygroscopic growth factor, optical parameters and enhancement parameters increase so substantial that the process become strongly nonlinear with relative humidity [25,73,77]. This effect is observed at different wavelengths, but for higher RH, the increase in AOT values is more evident at smaller wavelengths than longer wavelengths.

[4] The observed variations in Angstrom coefficients can be explained by changes in the effective radius of a mixture resulting from changes in RH and/or soot and water soluble concentrations: the larger the number of small aerosol particles, the smaller the effective radius and the larger the Angstrom coefficient. As a consequence of non-uniform increase in the optical depth with the increase in RH, the Ångström coefficient also becomes a function of RH, though at the delinquent points it decreases with the increase in RHs. This is because at the delinquent conditions the hygroscopic aerosols particles grow and this is what makes the Angstrom coefficients to decrease. However, the change in Angstrom coefficient due to variation in RH is more than that caused by differences in soot concentrations.

[5] The effect of RHs on asymmetric parameter shows that for smaller particles the hygroscopic growth increase forward scattering while for coarse particle it decreases forward scattering. It shows that increase in RH increases forward scattering because particle growth enhances forward diffraction Liou,[78]for smaller particles while in larger particles it causes increase in the backward scattering. It also shows that the mixture is internally mixed for smaller particles because of the increase in forward scattering as a result of the hygroscopic growth [79].

[6] These hygroscopic growth behaviors also reveal an immense potential of light scattering enhancement in the forward direction at high humidities and the potential for being highly effective cloud condensation nuclei for smaller particles.

[7] Finally, the data fitted our models very and can be used to extrapolate the hygroscopic growth and enhancements parameters at any RH. The values of R2 from the models show that Kelvin effects can be neglected.

REFERENCES

[1] IPCC (2007). Climate Change 2007: The Scientific Basis. In Solomon, S., Ding, Y., Griggs, D.G., Noguer, M., Vanderlinden, P.G., Dai, X., Maskell, K. and Johnson, C.A. (Eds). Contribution of Working Group I to the Fourth Assessment Report of the Intergovernmental Panel on Climate Change. Cambridge University Press. Cambridge.

[2] Li, W.F, Bai, Z.P., Liu, A.X., Chen, J. and Chen, L. (2009). Characteristics of Major PM2.5Components during Winter in Tianjin, China. Aerosol Air Qual. Res. 9: 105–119.

[3] Shen, Z.X., Cao, J.J, Tong, Z., Liu, S.X., Reddy, L.S.S., Han, Y.M, Zhang, T. and Zhou, J. (2009). Chemical Characteristics of Submicron Particles in Winter in Xi'an. Aerosol Air Qual. Res. 9: 80–93.

[4] Orr Jr. C., Hurd F. K., Corbett W. J., 1958, Aerosol size and relative humidity, J. Colloid Sci., 13, 472–482.

[5] Tang I. N., (1976), Phase transformation and growth of aerosol particles composed of mixed salts, J. Aerosol Sci., 7, 361–371.

[6] Swietlicki, E., Hansson, H.-C., Hameri, K., Svenningsson, B., Massling, A., et al.:(2008) Hygroscopic properties of submicrometer atmospheric aerosol particles measured with H-TDMA instru-ments in various environments – a review, Tellus B, 60(3), 432–469.

[7] Corrigan, C. E. and Novakov, T.: Cloud condensation nucleus activity of organic compounds: a laboratory study, Atmos. Environ., 33 (17), 2661–2668, 1999.

[8] Pitchford, M. L. and Mcmurry, P. H.: Relationship between Measured Water-Vapor Growth and Chemistry of Atmospheric Aerosol for Grand-Canyon, Arizona, in Winter 1990, Atmos. Environ., 28 (5), 827–839, 1994.

[9] Shulman, M. L., Jacobson, M. C., Charlson, R. J., Synovec, R. E., and Young, T. E.: Dissolution behavior and surface tension effects of organic compounds in nucleating cloud droplets (vol. 23, p. 277, 1996), Geophys. Res. Lett., 23 (5), 603–603, 1996.

[10] Swietlicki, E., Zhou, J. C., Berg, O. H., Martinsson, B. G., Frank, G., Cederfelt, S. I., Dusek, U., Berner, A., Birmili, W., Wiedensohler, A., Yuskiewicz, B., and Bower, K. N.: A closure study of sub-micrometer aerosol particle hygroscopic behaviour, Atmos. Res., 50 (3-4), 205–240, 1999.

[11] Hegg, D. A.: The importance of liquid phase oxidation of SO2 in the atmosphere, J. Geophys. Res., 90, 3773–3779, doi:10.1029/JD090iD02p03773, 1985.

[12] Blando, J. D. and Turpin, B. J.: Secondary organic aerosol formation in cloud and fog droplets: a literature evaluation of plausibility, Atmos. Environ., 34, 1623–1632, doi:10.1016/S1352-2310(99)00392-1, 2000.

[13] El Haddad, I., Yao Liu, Nieto-Gligorovski, L., Michaud, V., Temime-Roussel, B., Quivet, E., Marchand, N., Sellegri, K., and Monod, A.: In-cloud processes of methacrolein under simulated conditions – Part 2: Formation of secondary organic aerosol, Atmos. Chem. Phys., 9, 5107–5117, doi:10.5194/acp-9-5107-2009, 2009.

[14] Bateman, A. P., Nizkorodov, S. A., Laskin, J., and Laskin, A.: Photolytic processing of secondary organic aerosols dissolved in cloud droplets, Phys. Chem. Chem. Phys., 13, 12199–12212, doi:10.1039/c1cp20526a, 2011.

[15] Ervens, B., Turpin, B. J., and Weber, R. J.: Secondary organic aerosol formation in cloud droplets and aqueous particles (aqSOA): a review of laboratory, field and model studies, Atmos. Chem. Phys., 11, 11069–11102, doi:10.5194/acp-11-11069-2011, 2011.

[16] Ogren, J. A. and Charlson R. J.: Implications for models and measurements of chemical inhomogeneities among cloud droplets, Tellus, 44B, 489–504, 1992.

[17] Carrico, C. M., Rood, M. J., and Ogren, J. A.: Aerosol light scattering properties at Cape Grim, Tasmania, during the First Aerosol Characterization Experiment (ACE 1), J. Geophys. Res., 103(D13), 16565–16574, 1998.

[18] Carrico, C. M., Rood, M. J., Ogren, J. A., et al.: Aerosol Optical properties at Sagres, Portugal during ACE-2, Tellus B, 52(2), 694–715, 2000.

[19] Kotchenruther, R. A., Hobbs, P. V., and Hegg, D. A.: Humidification factors for atmospheric aerosols off the mid-Atlantic coast of the United States, J. Geophys. Res., 104(D2), 2239–2252, 1999.

[20] Randles , C. A. , Russell L. M. and. Ramaswamy V. (2004) Hygroscopic and optical properties of organic sea salt aerosol and consequences for climate forcing, Geophysical Research Letters, Vol. 31, L16108, doi:10.1029/2004GL020628.

[21] Crumeyrolle, S., Gomes, L., Tulet, P., Matsuki, A., Schwarzenboeck, A., and Crahan, K.: Increase of the aerosol hygroscopicity by cloud processing in a mesoscale convective system: a case study from the AMMA campaign, Atmos. Chem. Phys., 8, 6907–6924, 2008, http://www.atmos-chem-phys.net/8/6907/2008/.

[22] Houghton, J. T., Ding, Y., Griggs, D. J., et al.: IPCC, 2001: Climate Change 2001: The Scientific Basis. Contribution of Working Group I to the Third Assessment Report of the Intergovernmental Panel on Climate Change, Cambridge University Press, Cambridge, 2001.

[23] McMurry, P. and Stolzenburg, M.: On the sensitivity of particle size to relative humidity for Los Angeles aerosols, Atmos. Environ., 23, 497–507, 1989.

[24] Cocker, D., Whitlock, N., Flagan, R., and Seinfeld, J. H.: Hygroscopic properties of Pasadena, California aerosol, Aerosol Sci. Technol, 35, 2, 637–647, 2001.

[25] Tang I.N., (1996) Chemical and size effects of hygroscopic aerosols on light scattering coefficient, J. Geophys. Res., 101(D14),19245–19250.

[26] Cruz, C. N. and Pandis, S. N.: Deliquescence and Hygroscopic Growth of Mixed Inorganic-Organic Atmospheric Aerosol, Environ. Sci. Technol., 34(20), 4313–4319, 2000.

[27] Kim, J., Yoon, S. C., Jefferson, A., et al.: Aerosol hygroscopic properties during Asian dust, pollution, and biomass burning episodes at Gosan, Korea in April 2001, Atmos. Environ., 40(8), 1550–1560, 2006.

[28] Hand, J. L. and Malm, W. C.: Review of the IMPROVE Equation for Estimating Ambient Light Extinction Coefficients-Final Report, 47, 2006.

[29] Li-Jones, X., Maring, H. B., and Prospero, J. M.: Effect of relative humidity on light scattering by mineral dust aerosol as measured in the marine boundary layer over the tropical Atlantic Ocean, J. Geophys. Res., 103(D23), 31113-31121, 1998.

[30] Perry, K. D., Cliff, S. S., and Jimenez-Cruz, M. P.: Evidence for hygroscopic mineral dust particles from the Intercontinental Transport and Chemical Transformation Experiment, J. Geophys. Res., 109, D23S28, doi:10.1029/2004JD004979, 2004.

[31] Shi, Z., Zhang, D., Hayashi, M., et al.(2007): Influences of sulfate and nitrate on the hygroscopic behaviour of coarse dust particles, Atmos. Environ., 42(4), 822–827.

[32] Randall, D. A., Wood, R. A., Bony, S., Colman, R., Fichefet, T., Fyfe, J., Kattsov, V., Pitman, A., Shukla, J., Srinivasan, J., Stouffer, R. J., Sumi, A., and Taylor, K. E.: Contribution of Working Group I to the Fourth Assessment Report of the Intergovernmen-tal Panel on Climate Change – Climate Models and their Evalua-tion, Cambridge University Press, Cambridge, United Kingdom and New York, 589–662, 2007.

[33] Yan, P., Pan, X. L., Tang, J., Zhou, X. J., Zhang, R. J., and Zeng, L. M.: Hygroscopic growth of aerosol scattering coefficient: a comparative analysis between urban and suburban sites at winter in Beijing, Particuology, 7, 52–60, 2009.

[34] Fitzgerald, J. W., Hoppel, W. A., and Vietti, M. A.: The size and scattering coefficient of urban aerosol particles at Washington, DC as a function of relative humidity, J. Atmos. Sci., 39, 1838–1852, 1982.

[35] Jeong M. J, Li Z., Andrews E., Tsay S. C., (2007) Effect of aerosol humidification on the column aerosol optical thickness over the Atmospheric Radiation Measurement Southern Great Plains site, J. Geophys. Res., 112, D10202, doi:10.1029/2006JD007176.

[36] Rapti A.S., (2005) Spectral optical atmospheric thickness dependence on the specific humidity in the presence of continental and marine air masses, Atmos. Res., 78(1–2),13–32.

[37] Hess M., Koepke P., and Schult I (May 1998), Optical Properties of Aerosols and Clouds: The Software Package OPAC, Bulletin of the A merican Met. Soc. 79, 5, p831-844.

[38] Sjogren, S., Gysel, M., Weingartner, E., Baltensperger, U., Cubi-son, M. J., Coe, H., Zardini, A. A., Marcolli, C., Krieger, U. K., and Peter, T.: Hygroscopic growth and water uptake kinetics of two-phase aerosol particles consisting of ammonium sulfate, adipic and humic acid mixtures, J. Aerosol Sci., 38, 157–171, doi:10.1016/j.jaerosci.2006.11.005, 2007.

[39] Stokes, R. H. and Robinson, R. A.: Interactions in aqueous nonelec-trolyte solutions. I. Solute-solvent equilibria, J. Phys. Chem., 70, 2126–2130, 1966.

[40] Meyer, N. K., Duplissy, J., Gysel, M., Metzger, A., Dommen, J., Weingartner, E., Alfarra, M. R., Prevot, A. S. H., Fletcher, C., Good, N., McFiggans, G., Jonsson,˚ A. M., Hallquist, M., Baltensperger, U., and Ristovski, Z. D.: Analysis of the hy-groscopic and volatile properties of ammonium sulphate seeded and unseeded SOA particles, Atmos. Chem. Phys., 9, 721–732, doi:10.5194/acp-9-721-2009, 2009.

[41] Stock M., Y. F. Cheng, W. Birmili, A. Massling, B. Wehner, T. Muller, S. Leinert, N. Kalivitis,N. Mihalopoulos, and A. Wiedensohler, Hygroscopic properties of atmospheric aerosol particles over the Eastern Mediterranean: implications for regional direct radiative forcing under clean and polluted conditions, Atmos. Chem. Phys., 11, 4251–4271, 2011 www.atmos-chem-phys.net/11/4251/2011/ doi:10.5194/acp-11-4251-2011

[42] Duplissy J., P. F. DeCarlo, J. Dommen, M. R. Alfarra, A. Metzger, I. Barmpadimos, A. S. H. Prevot, E. Weingartner, T. Tritscher, M. Gysel, A. C. Aiken, J. L. Jimenez, M. R. Canagaratna , D. R. Worsnop, D. R. Collins, J. Tomlinson, and U. Baltensperger, (2011) Relating hygroscopicity and composition of organic aerosol particulate matter Atmos. Chem. Phys., 11, 1155–1165, www.atmos-chem-phys.net/11/1155/2011/ doi:10.5194/acp-11-1155-2011.

[43] Meier J., B. Wehner, A. Massling, W. Birmili, A. Nowak, T. Gnauk, E. Bruggemann, H. Herrmann, H. Min, and A. (2009)Wiedensohler Hygroscopic growth of urban aerosol particles in Beijing (China) during wintertime: a comparison of three experimental methods, Atmos. Chem. Phys., 9, 6865–6880, www.atmos-chem-phys.net/9/6865/2009.

[44] Petters, M. D. and Kreidenweis, S. M. (2007). A single parameter representation of hygroscopic growth and cloud condensation nucleus activity. Atmos. Chem. Phys. 7(8): 1961–1971.

[45] Christensen, S. I. and Petters, M. D. (2012). Th e role of temperature in cloud droplet activation. J. Phys. Chem. A 116(39): 9706–9717.

[46] Liu P. F., Zhao C. S., Gobel T., Hallbauer E., Nowak A., Ran L., Xu W. Y., Deng Z. Z., Ma N., Mildenberger K., Henning S., Stratmann F., and Wiedensohler A. (2011) Hygroscopic proper ties of aerosol par ticles at high relative humidity and their diurnal variations in the Nor th China Plain, Atmos. Chem. Phys. Discuss., 11, 2991–3040

[47] Swietlicki, E., Zhou, J., Covert, D. S., Hameri, K., Busch, B., Vakeva, M., Dusek, U., Berg, O. H., Wiedensohler, A., Aalto, P., Makela, J., Martinsson, B. G., Papaspiropoulos, G., Mentes, B., Frank, G., and Stratmann, F.: Hygroscopic properties of aerosol particles in the northeastern Atlantic during ACE-2, Tellus, 52B, 201–227, 2000.

[48] Birmili, W., Nowak, A., Schwirn, K., Lehmann, K.et al. (2004) A new method to accurately relate dry and humidified number size distributions of atmospheric aerosols. Journal of Aerosol Science 1, 15–16, Abstracts of EAC, Budapest 2004.

[49] Kasten, F.: Visibility forecast in the phase of pre-condensation, Tel-lus, XXI, 5, 631–635, 1969.

[50] Gysel, M., McFiggans, G. B., and Coe, H.: Inversion of tandem differential mobility analyser (TDMA) measurements, J. Aerosol Sci., 40, 134–151, 2009.

[51] Putaud, J. P. (2012): Interactive comment on "Aerosol hygroscopicity at Ispra EMEP-GAW station" by M. Adam et. al., Atmos. Chem. Phys. Discuss., 12, C1316–C1322.

[52] Doherty, et al., 2005. A comparison and summary of aerosol optical properties as observed in situ from aircraft, ship, and land during ACE-Asia. Journal of Geophysical Research 110, D04201.

[53] Quinn, P. K., et al. (2005) , Impact of particulate organic matter on the relative humidity dependence of light scattering: A simplified parameterization, Geophys. Res. Lett., 32, L22809, doi:10.1029/2005GL024322.

[54] Gasso S., et al. (2000), Influence of humidity on the aerosol scattering coefficient and its effect on the upwelling radiance during ACE-2, Tellus, Ser. B , 52, 546 – 567.

[55] Clarke, A., et al. (2007), Biomass burning and pollution aerosol over North America: Organic components an d their influence on spectral optical properties and humidification response, J. Geophys. Res., 11 2, D12S18, doi:10.1029/2006JD007777.

[56] Hanel, G. (1976). The Properties of Atmospheric Aerosol Particles as Functions of Relative Humidity at Thermodynamic Equilibrium with Surrounding Moist Air.InAdvances in Geophysics, Vol. 19 , H. E. Landsberg and J. Van Mieghem, eds., Academic Press, New York, pp. 73–188.

[57] Angstrom, A.(1961): Techniques of Determining the Turbidity of the At-mosphere, Tellus, 13, 214–223.

[58] King, M. D. and Byrne, D. M.: A method for inferring total ozone content from spectral variation of total optical depth obtained with a solar radiometer, J. Atmos. Sci., 33, 2242–2251, 1976.

[59] Eck, T. F., Holben, B. N., Reid, J. S., Dubovic, O., Smirnov, A., O'Neil, N. T., Slutsker, I., and Kinne, S.: Wavelength dependence of the optical depth of biomass burning, urban, and desert dust aerosols, J. Geophys. Res., 104(D24), 31 333–31 349, 1999.
[60] Eck, T. F., Holben, B. N., Dubovic, O., Smirnov, A., Slutsker, I., Lobert, J. M., and Ramanathan, V.: Column-integrated aerosol optical properties over the Maldives during the northeast mon-soon for 1998–2000, J. Geophys. Res., 106, 28 555–28 566, 2001a.
[61] Eck, T. F., Holben, B. N., Ward, D. E., Dubovic, O., Reid, J. S., Smirnov, A., Mukelabai, M. M., Hsu, N. C., O' Neil, N. T., and Slutsker, I.: Characterization of the optical properties of biomass burning aerosols in Zambia during the 1997 ZIBBEE field campaign, J. Geophys. Res., 106(D4), 3425–3448, 2001b.
[62] Kaufman, Y. J., Aerosol optical thickness and atmospheric path radiance, J. Geophys. Res., 98, 2677-2992, 1993.
[63] O'Neill, N. T., Dubovic, O., and Eck, T. F.(2001): Modified Angstrom exponent for the characterization of submicrometer aerosols, Appl. Opt., 40(15), 2368–2375.
[64] O'Neill, N. T., Eck, T. F., Smirnov, A., Holben, B. N., and Thulasiraman, S.: Spectral dis-crimination of coarse and fine mode optical depth, J. Geophys. Res., 198(D17), 4559, doi:101029/2002JD002975, 2003.
[65] Pedros, R., Martinez-Lozano, J. A., Utrillas, M. P., Gomez-Amo, J. L., and Tena, F.(2003): Column-integrated aerosol, optical properties from ground-based spectroradiometer measurements at Barrax (Spain) during the Digital Airborne Imaging Spectrometer Experiment (DAISEX) campaigns, J. Geophys. Res., 108(D18), 4571, doi:10.1029/2002JD003331.
[66] Kaskaoutis, D. G. and Kambezidis, H. D.(2006): Investigation on the wavelength dependence of the aerosol optical depth in the Athens area, Q. J. R. Meteorol. Soc., 132, 2217–2234.
[67] Schmid, B., Hegg, D.A., Wang, J., Bates, D., Redemann, J., Russell, P.B., Livingston, J.M., Jonsson, H.H., Welton, E.J., Seinfeld, J.H., Flagan, R.C., Covert, D.S., Dubovik, O., Jefferson, A., (2003). Column closure studies of lower tropospheric aerosol and water vapor during ACE-Asia using airborne Sun photometer and airborne in situ and ship-based lidar measurements. Journal of Geophysical Research 108 (D23), 8656.
[68] Martinez-Lozano, J.A., Utrillas, M.P., Tena, F., Pedros, R., Canada, J., Bosca, J.V., Lorente, J., (2001). Aerosol optical characteristics from summer campaign in an urban coastal Mediterranean area. IEEE Transactions on Geoscience and Remote Sensing 39, 1573–1585.
[69] Aspens D. E. (1982), Local-field effect and effective medium theory: A microscopic perspective Am. J. Phys. 50, 704-709.
[70] Lorentz, H. A. (1880). Ueber die Beziehungzwischen der Fortpflanzungsgeschwindigkeit des Lichtes und der Korperdichte. Ann. P hys. Chem. 9, 641–665.
[71] Lorenz, L. (1880). Ueber die Refractionconstante. Ann. P hys. Chem. 11, 70–103.
[72] Schuster, G.L., Dubovik, O. and Holben, B.N. (2006). Angstrom Exponent and Bimodal Aerosol Size Distributions. J. Geophy. Res. 111: 7207.
[73] Fitzgerald , J. W. (1975) Approximation formulas for the equilibrium size of an aerosol particle as a function of its dry size and composition and ambient relative humidity. J. Appl .Meteorol. , 14, 1044 –1049.
[74] Sheridan, P. J., Delene D. J., and Ogren J. A. (2001), Four years of continuous surface aerosol measurements from the Department of Energy's Atmospheric Radiation Measurement Program Southern Great Plains Cloud and Radiation Testbed site,J. Geophys. Res., 106, 20,735–20,747.
[75] Whitby, K. (1978), The physical characteristics of sulfur aerosols, Atmos. Environ., 12, 135–159.
[76] Seinfeld, J., and S. Pandis (1998), Atmospheric Chemistry and Physics: From Air Pollution to Climate Change, Wiley.
[77] Kuśmierczyk-Michulec, J. (2009). Ångström coefficient as an indicator of the atmospheric aerosol type for a well- mixed atmospheric boundary layer: Part 1: Model development. Oceanologia , Vol. 51, p. 5-39.
[78] Liou, K. N. (2002), An Introduction ro Atmospheric Radiation, 583pp., Elsevier, New York.
[79] Wang, J., and S. T. Martin (2007), Satellite characterization of urban aerosols: Importance of including hygroscopicity and mixing state in the retrieval algorithms, J. Geophys. Res., 112 , D 17203, doi:1 0.1029 /2006JD008078.